Laboratory Investigation (2017) 97, 356–369

The role of endothelial HIF-1α in the response to sublethal hypoxia in C57BL/6 mouse pups

Qi Li[1], Michael Michaud[1], Chan Park[1,2], Yan Huang[3], Rachael Couture[4], Frank Girodano[3], Michael L Schwartz[4] and Joseph A Madri[1]

Chronic sublethal hypoxia, a complication of premature birth, is associated with cognitive and motor handicaps. Responsiveness to and recovery from this hypoxic environment is dependent on induction of HIF-1α in the cells affected. Microvascular endothelial–glial and microvascular endothelial–neuronal precursor interactions have been found to be dynamic and reciprocal, involving autocrine and paracrine signaling, with response and recovery correlated with baseline levels and levels of induction of HIF-1α. To ascertain the roles of endothelial HIF-1α in the responses of brain microvascular endothelial cells (EC) and neuronal precursors to hypoxia, we examined the effects of the presence and absence of endothelial HIF-1α expression in culture and in cells comprising the subventricular zone (SVZ) and dentate gyrus under normoxic and hypoxic conditions. We used C57BL/6 WT and EC HIF-1α-deficient mice and brain microvascular ECs isolated from these mice in western blots, immunofluorescence, and behavioral studies to examine the roles of EC HIF-1α behaviors of endothelial and neuronal precursor cells (NPCs) in SVZ and hippocampal tissues under normoxic and hypoxic conditions and behaviors of these mice in open field activity tests. Analyses of ECs and SVZ and dentate gyrus tissues revealed effects of the absence of endothelial HIF-1α on proliferation and apoptosis as well as open field activity, with both ECs and neuronal cells exhibiting decreased proliferation, increased apoptosis, and pups exhibiting gender-specific differences in open field activities. Our studies demonstrate the autocrine and paracrine effects of EC HIF-1α-modulating proliferative and apoptotic behaviors of EC and NPC in neurogenic regions of the brain and gender-specific behaviors in normoxic and hypoxic settings.
Laboratory Investigation (2017) **97,** 356–369; doi:10.1038/labinvest.2016.154; published online 16 January 2017

Chronic sublethal hypoxia is a well-known complication of very premature birth and is associated with cognitive and motor handicaps, many of which can persist throughout the life of the infant.[1–8] Responsiveness to and recovery from this hypoxic (Hx) environment is in good part dependent on induction of HIF-1α in the cells affected.[2,3] The central nervous system's responses to Hx insult are multicellular, encompassing neuronal precursors (NPCs), neurons, astrocytes, glia, and endothelial cells (ECs).[2,9–14] In previous *in vitro* models, we have examined microvascular endothelial–glial and microvascular endothelial–neuronal precursor interactions and found both of these intimate interactions to be dynamic and reciprocal in nature, involving autocrine[15–18] and paracrine signaling.[11–13,19–23] In our studies, we have observed that the levels of response and recovery in both our *in vitro* and *in vivo* models of chronic sublethal hypoxia of the premature newborn correlate, in part, with the levels of induction of Sox 10, BDNF, VEGF, EPO, and HIF-1α in neuronal precursors and microvascular ECs in the subventricular zone (SVZ) and cognitive behavior in selected strains (CD1 and C57BL/6).[10,24] Specifically, neuronal precursors and microvascular ECs derived from a particular strain (CD1), exhibit greater HIF-1α baseline and induction, also exhibit a more robust recovery compared with another strain (C57BL/6), which exhibit a lower baseline, a more modest induction of Sox 10, and only minimal induction to modestly decreased expression of HIF-1α and the above-mentioned genes.[2,3] In a recent study, we found that using a tetracycline (minocycline) known for its noncanonical effects, we were able to affect the increase in the levels of Sox 10 in C57BL/6 brain ECs, which in turn elicited increases in HIF-1α levels and improvement of cognitive behavior in C57BL/6 mice.[24]

[1]Department of Pathology, Yale University School of Medicine, New Haven, CT, USA; [2]Sungkyunkwan University School of Medicine, Seoul, South Korea; [3]Department of Cardiovascular Medicine, Yale University School of Medicine, New Haven, CT, USA and [4]Department of Neuroscience, Yale University School of Medicine, New Haven, CT, USA

Correspondence: Professor JA Madri, PhD, MD, Department of Pathology, Yale University School of Medicine, 310 Cedar Street, LH 115A, New Haven, CT 06520, USA. E-mail: joseph.madri @yale.edu

Received 7 October 2016; revised 4 December 2016; accepted 7 December 2016

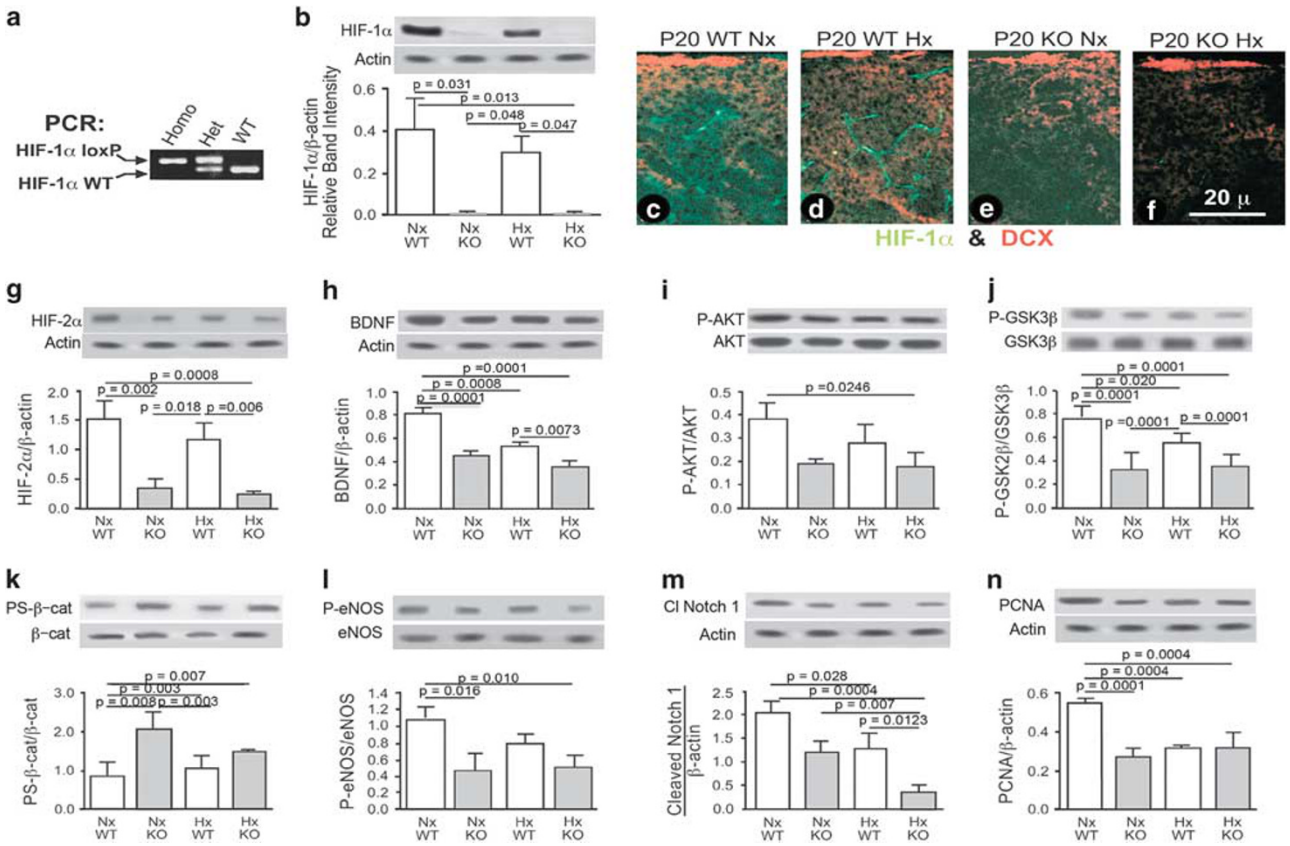

Figure 1 Endothelial cells deficient in HIF-1*α* (HIF-1*α* EC-KO cells) exhibit lower levels of: HIF-2*α*, BDNF, phospho (p)-AKT, p-eNOS, inactive GSK-3*β*, increased p-*β*-catenin and decreased P-eNOS, cleaved Notch 1, and PCNA. (**a**) Representative PCR analysis of homozygous (Homo), heterogygous (Het) and wild-type (WT) pups illustrating the presence of HIF-1α in WT and its absence of the HIF-1α EC KO. (**b**) Quantitative western blot analysis of cultured WT and KO endothelial cell lysates illustrating the presence (WT) and absence (KO) of HIF-1α protein expression under both normoxic (Nx) and reduced O_2 (Hx) conditions. Horizontal lines denote statistical significance with *P*-values inserted above $n = 3$. (**c–f**) Representative immunofluorescence micrographs of P20 SVZ tissues labeled with anti-HIF-1α and doublecortin (DCX): (**c**) WT Nx; (**d**) WT Hx; (**e**) KO Nx; (**f**) KO Hx. Scale bar = 20 *μ*. (**g-n**) Quantitative western blot analyses of cultured WT and KO endothelial cell lysates cultured under Nx and Hx conditions illustrating the of levels of: (**g**) HIF-2α (HIF-1α/*β*-actin); (**h**) BDNF (BDNF/*β*-actin); (**i**) P-Akt (P-akt/Akt); (**j**) P-GSK-3*β*-S9 (P-GSK-3*β*-S9/GSK-3*β*); (**k**) PS-*β*-catenin (PS-*β*-catenin/*β*-catenin); (**l**) P-eNOS (P-eNOS/eNOS); (**m**) cleaved Notch 1 (cleaved Notch 1/*β*-actin); (**n**) PCNA (PCNA/*β*-actin). Values represent averages of three independent determinations. Horizontal lines denote statistical significance with *P*-values of < 0.05. Representative western blots of each of the quantitative western blot analyses are illustrated above each western analysis panel. BDNF, brain-derived neurotrophic factor; EC, endothelial cell; eNOS, endothelial constitutive nitric oxide synthase; GSK-3*β*, glycogen synthase kinase-3*β*; HIF-1α, hypoxia-inducible factor 1-α, KO, knockout; PCNA, proliferating cell nuclear antigen.

In light of our previous findings,[2,3,10,12,24] we now examine the effects of the presence and absence of EC HIF-1***α*** expression in the SVZ ECs and neuronal progenitors of C57BL/6 mice under normoxic (Nx) and reduced oxygen conditions, mimicking the chronic sublethal hypoxia of the very premature newborn. In the studies described here, we explored the possibility that endothelial HIF-1***α*** affects not only local EC populations in autocrine and paracrine manners but also affects local neuronal cells with also comprise neurovascular and neurogenic niches. Our results, using C57BL/6 pups, tissues, and cells, illustrates that endothelial HIF-1***α*** deficiency results in a decrease of HIF-1***α*** in the SVZ tissues and decreased expression levels of HIF-2***α***, Sox 10, Sox 2, EPO, BDNF, c-Myc, cleaved Notch 1, P-eNOS, PCNA, YAP and S_9P-GSK-3*β*, Survivin, Gpr124, and CD31 and increases in cleaved caspase-3, consistent with losses of endothelial and neuronal cell densities, decreased proliferation, and increased apoptosis in both endothelial and neuronal populations in the SVZ and hippocampus and gender-specific changes in behavioral profiles of the endothelial HIF-1***α***-deficient mice.

MATERIALS AND METHODS

Mice

All animal experiments were conducted in accordance with the NIH Guide on the Care and Use of Laboratory Animals and in compliance with the Yale University animal care committee regulations (approved protocol no. 07366). All efforts were made to minimize suffering.

EC-specific inactivation of HIF-1***α*** was achieved by cross-breeding Tie2-Cre transgenic mice[25] with HIF-1$\alpha^{+f/+f}$ mice homozygous for the HIF-1*α* allele with exon 2 flanked by

loxp sites.[26] HIF-1α EC knockout (KO) mice, heterozygous mice, and wild-type (WT) littermates were confirmed by PCR using the forward (sense) and reverse (antisense) primers 5′-GGAGCTATCTCTCTA GACC-3′ (712–730) and 5′-CGA GTTAAGAGCACTAGTTG-3′ (929–909) for the HIF-1α loxP allele and using the forward (sense) and reverse (antisense) primers: sense strand, 5′-CGCATAACCAGTGAAACAGCA TTGC-3′ and antisense strand, 5′-CCCTGTGCTCAGACAG AAATGAGA-3′, respectively, for the Tie2-Cre allele. Homozygous pups exhibit one band (HIF-1α loxP); heterozygous pups exhibit two bands: one higher band (identical to HIF-1a loxP) and a lower band (HIF-1α WT); WT pups exhibit one band: (HIF-1α WT) (Figure 1a). In all experiments, littermates from the same breeding pairs were used as controls.

Animals

Timed-pregnant litters and associated dams were kept in Nx conditions (20% O_2) from birth (postnatal day 0 (P0)) until P3. The litters in each cage typically contained seven to eight C57BL/6 pups. At P3, one-half of the litters were placed in a hypoxia chamber at 10% O_2 from P3 to P11, whereas the other half were maintained in Nx (20% O_2) as described previously.[2,3] This period of brain development in mice corresponds to ~23 weeks of gestation to full term in the humans.[3,9,27] At P11, the litters were removed from the reduced O_2 environment and placed in ambient oxygen conditions (20% O_2). Pups were harvested at P10 and P20 for immunofluorescence and western blotting studies. Other pups underwent behavioral testing at P20 (open field activity).

Tissues

SVZ tissues were isolated from WT and homozygous mice at P20 and prepared for immunofluorescence and western blot analyses as described previously.[24]

Cells

Brain microvascular WT ECs were derived, cultured, and passaged from WT C57BL/6 P0 pup brains as described previously.[24,28] At confluency, cultures were placed in humidified chambers at either 20% O_2 (Nx) or 10% O_2 (Hx) for 3 days, following which lysates were prepared as described previously.[11,12]

Reagents

All antibodies used in this study, the vendors, and their locations are listed in Supplementary Table 1. All antibodies were used at a 1:1000 dilution for western blots and 1:100 or 1:200 dilutions for immunofluorescence.

Biochemical and Morphological Studies

At P10 and P20 three pups from each condition were anesthetized, perfused with sterile PBS, and their brains removed. The harvested brains were weighed and total cerebral hemispheres or dissected SVZ tissues were prepared for western blotting following lysis as described previously.[12]

Immunofluorescence

Ten micron frozen sections of P10 and P20 SVZ were prepared and stained with antibodies as described.[24] Briefly, three pups from each condition were anesthetized and then perfused with sterile PBS, followed by 4% paraformaldehyde in sterile PBS. Brains were then placed in 10% to 20% to 30% over 3 days, placed on chucks with OCT, and sectioned at 10 μ on a Reichert microtome as described previously.[2,3,11,12] Sections of SVZ were stained for Ki67, cleaved caspase-3, CD31, PCNA, YAP, Sruvivin, and DAPI. Sections of cerebrum were stained for HIF-1a, doublecortin (DCX), GFAP, Ki67, and DAPI. Tissue sections were analyzed using an Olympus IX 71 inverted fluorescence/phase and bright field microscope (Olympus, Tokyo, Japan) equipped with an Optronics Microfire camera (Goleta, CA, USA) and Pictureframe version

Figure 2 HIF-1α EC-KO SVZ tissues exhibit decreased Ki67, increased cleaved caspase-3, and decreased CD31 in the SVZ. (**a–d**) Representative fluorescence microscopic micrographs of SVZ tissues revealed decreases in Ki67 labeling in normoxic wild-type (Nx WT) and Nx and Hx knockout (Nx and Hx KO) SVZ compared with NX WT SVZ tissues. Scale bar = 100 μm. (**e**) Quantitation of the numbers of Ki67-positive cells in the SVZ tissues derived from analysis of the SVZ of three pups. Horizontal lines denote statistical significance with *P*-values of <0.05. (**f**) Western blot analysis of NX and HX WT and KO SVZ tissues derived from three pups, labeling with PCNA antibody, confirming the morphological-based results. Horizontal lines denote statistical significance with *P*-values of <0.05, $n=3$. (**g**) Representative high-power micrographs illustrating the differences noted in WT Nx SVZ compared with KO Nx SVZ. Scale bar = 50 μm. (**h-k**) Representative fluorescence microscopic micrographs of SVZ tissues revealed increases in cleaved caspase-3 (CC3) labeling in Hx WT and Nx and Hx KO SVZ compared with Nx WT SVZ tissues. Scale bar = 100 μm. (**l**) Quantitation of the numbers of CC3-positive cells in the SVZ tissues derived from analysis of the SVZ of three pups. Horizontal lines denote statistical significance with *P*-values of <0.05. (**m**) Western blot analysis of Nx and Hx WT and KO SVZ tissues derived from three pups, labeling with cleaved caspase-3 antibody, confirming the morphological-based results. Horizontal lines denote statistical significance with *P*-values of <0.05, $n=3$. (**n**) Representative high-power micrographs illustrating the differences noted in Nx WT SVZ compared with Nx KO SVZ. Scale bar = 50 μm. (**o–r**) Representative fluorescence microscopic micrographs of SVZ tissues revealed decreases in CD31 labeling in Hx WT and Hx KO SVZ compared with Nx WT and KO SVZ tissues. Scale bar = 100 μm. (**s**) Quantitation of CD31-positive tube length in the SVZ tissues derived from the analysis of the SVZ of three pups. Horizontal lines denote statistical significance with *P*-values of <0.05. (**t**) Western blot analysis of Nx and Hx WT and KO SVZ tissues derived from three pups, labeling with CD31 antibody, confirming the morphological-based results. Horizontal lines denote statistical significance with *P*-values of <0.05, $n=3$. (**u**) Representative high-power micrographs illustrating the differences noted in WT Nx SVZ compared with KO Nx SVZ. Scale bar = 50 μm. Representative western blots of each of the quantitative western blot analyses are illustrated above each western analysis panel. EC, endothelial cell; KO, knockout; PCNA, proliferating cell nuclear antigen; SVZ, subventricular zone.

3.00.30 software. Photoshop CS6 (Adobe Systems, San Jose, CA, USA) and InDesign CS6 (Adobe Systems) were used to generate publication micrographs as described previously.[29,30]

Western Blotting

SVZ regions were dissected out of the brains of pups from each condition and homogenized in a lysis buffer as described.[2,3,11,12] All data obtained from western blot analyses were reported as averages of three independent analyses. Statistical significance (determined using *N*-way analysis of variance) was ascribed to the data that achieved $P<0.05$ (expressed as means ± s.d.) using the StatView statistical package on a Macintosh G5 computer. Specifically, *N*-way analysis of variance was used to evaluate the statistical significance of comparisons of western blots of Nx and reduced oxygen-treated NSC cultures. *N*-way analysis of

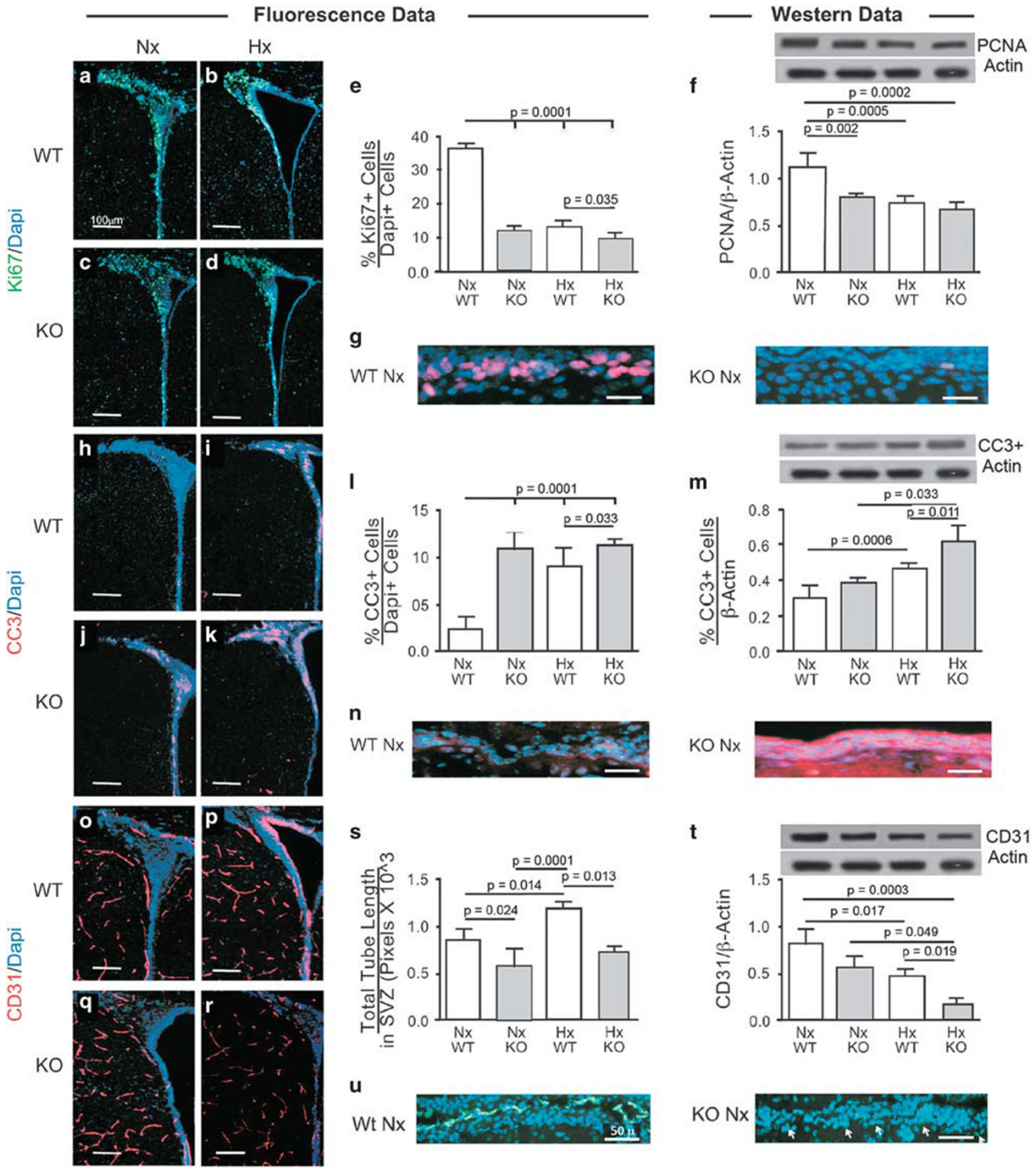

variance was also used in examination of western blots of SVZ isolated from P10 and P20 pups reared under Nx and reduced oxygen levels.

Behavioral Testing

Open field activity

At P20, mice were assessed using the open field activity task as described previously.[24] Thirty-seven male and female P20 pups (20 HIF-1α EC-KO and 17 WT C57BL/6 littermate pups, comprised of 18 Nx-reared and 19 Hx-reared pups totaling to 17 males—8 Nx and 9 Hx males and 20 females—10 Hx and 10 Nx females) were evaluated for spontaneous open field behavior. Mice were placed in a Plexiglas-enclosed open field ($25 \times 25 \times 40\ cm^3$) equipped with infrared photo beams coupled to a computer running TruScan software version 2.06-USB (Coulbourn Instruments, Whitehall, PA, USA) to automatically record movements within the field. Activity was monitored during a single 15-min session and measures of total distance moved (centimeters per 3 min), the mean velocity of movements (coordinate changing movements), the amount of time without movement (rest time; seconds per 3 min), margin time (time within 3.8 cm of the chamber wall), and center time (time central to the area within 3.8 cm of the chamber wall) were recorded. Data were binned into three 3-min intervals and were analyzed using a multiple analysis of variance test with repeated measures. At least three mice comprised of each group studied. Statistical significance (determined by *N*-way analysis of variance) were ascribed to the data that achieved $P < 0.05$ expressed as means ± s.d. using the StatView program version 5 (SAS Institute, Cary, NC, USA) in the Excel:mac 2011 statistical package version 14.3.8 on a Macintosh G5 computer (Apple, Cupertino, CA, USA).

RESULTS

C57BL/6 HIF-1α EC-KO Mice do not Express Endothelial HIF-1α

Offspring of matings of Tie2-Cre transgenic mice and HIF-$1\alpha^{+f/+f}$ mice homozygous for the HIF-1α allele with exon 2 flanked by loxP sites were analyzed by PCR at 3 weeks of age and identified by numbered ear tags. Animals homozygous for HIF-1α loxP yielded a single band, whereas heterozygous animals exhibited two bands and WT animals yielded a single lower band (Figure 1a). The absence of HIF-1α was confirmed in cultures of WT and HIF-1α KO ECs by western blotting with no detectable HIF-1α. P20 SVZ tissue sections examined using antibodies directed against HIF-1α and DCX immunofluorescence revealed vascular HIF-1α labeling in both Nx- and Hx WT-reared pup tissues (Figures 1c and d) and a lack of vascular labeling in Nx- and Hx-reared KO pup SVZ tissues (Figures 1e and f).

HIF-1α EC-KO EC Express Lower Levels of: BDNF, p-AKT, p-eNOS, Inactive GSK-3β, and Increased p-β-catenin

Western blot analysis of WT and KO EC cultured under Nx (20% O_2) and reduced oxygen (Hx) (10% O_2) conditions revealed significant reductions in HIF-2α in the Nx and reduced O_2 KO cultures (Figure 1g). Analysis of BDNF revealed significant loss in BDNF expression in Nx and reduced O_2-cultured KO EC and a similar reduction in reduced O_2-cultured WT EC compared with Nx-cultured WT EC (Figure 1h). Similar reductions were also observed in the fractions of phospho-Akt compared with total Akt (Figure 1i), as well as the fractions of P-GSK-3β(S9) when compared with total GSK-3β1J. When the fractions of PS-β-catenin were compared with total β-catenin, both Nx and reduced O_2 KO EC exhibited higher fractions of PS-β-catenin compared with both Nx and reduced O_2 WT EC cultures (Figure 1k). When the fractions of P-eNOS were compared with total eNOS (Figure 1l), they were found to be decreased compared with Hx WT, Nx KO, and Hx KO cultures. Similarly, levels of cleaved Notch 1 and PCNA were also found to be reduced in Hx WT, Nx KO, and Hx KO cultures compared with Nx WT cultures (Figures 1m and n). Representative western blots used in the quantitation of the proteins listed in Figure 1 are illustrated below each panel. Supplementary Table 2A is a compilation of the statistical analyses performed on results of the western blots. Supplementary Table 2B is a summary of the statistical analyses illustrated in Supplementary Table 2A and illustrates the general patterns of gene differences in Nx KO *vs* Hx WT and Nx KO *vs* Hx KO compared with Nx WT *vs* Nx KO, Nx WT *vs* Hx WT, Hx WT *vs* Hx KO, and Hx WT *vs* Hx KO, consistent with differences in the pathways impacted by the various combinations of O_2% and HIF-1α EC KO affecting the ECs. In general, when Nx KO, Hx WT, and Hx KO were compared with Nx WT, the KO and Hx samples exhibited decreased expression of genes associated with EC proliferation. In contrast, Nx KO, HX WT, and Hx KO samples exhibited no differences in the decreases in expression of these genes, consistent with decreased proliferation.

HIF-1α EC-KO SVZ Tissues Exhibit Decreased Ki67, Increased Cleaved Caspase-3, and Decreased CD31

Immunofluorescence analysis of P10 WT and HIF-1α EC-KO SVZ tissues revealed increased Ki67 labeling in Nx WT pup tissues compared with WT pups reared in reduced O_2 and KO pups reared in both Nx and reduced O_2 conditions (Figures 2a–d). Quantitation of Ki67-positive SVZ cells reared in these conditions is illustrated in Figure 2e, consistent with panels a–d. Figure 2f represents the summary of three independent western blot analyses of SVZ tissue lysates analyzed for PCNA expression, confirming the morphological data illustrated in Figures 2a–e. Above the quantitation of the western blot analysis is a representative micrograph of the immunoblots. Figure 2g is comprised of two high-power micrographs of SVZ areas illustrating the increased Ki67 labeling in WT Nx-reared pups compared with the greatly diminished labeling in KO pups reared in Nx conditions. Diminished Ki67 labeling was also noted in WT and KO pups reared in reduced O_2 conditions (not shown).

Immunofluorescence analysis of P10 WT and HIF-1α KO KO SVZ tissues revealed increased cleaved caspase-3 labeling in WT pups reared in reduced O_2 and KO pups reared in Nx and reduced O_2 conditions compared with WT pups reared in Nx conditions (Figures 2h–k). Quantitation of cleaved caspase-3-positive SVZ cells reared in these conditions is illustrated in Figure 2l. Figure 2m represents the summary of three independent western blot analyses of SVZ tissue lysates analyzed

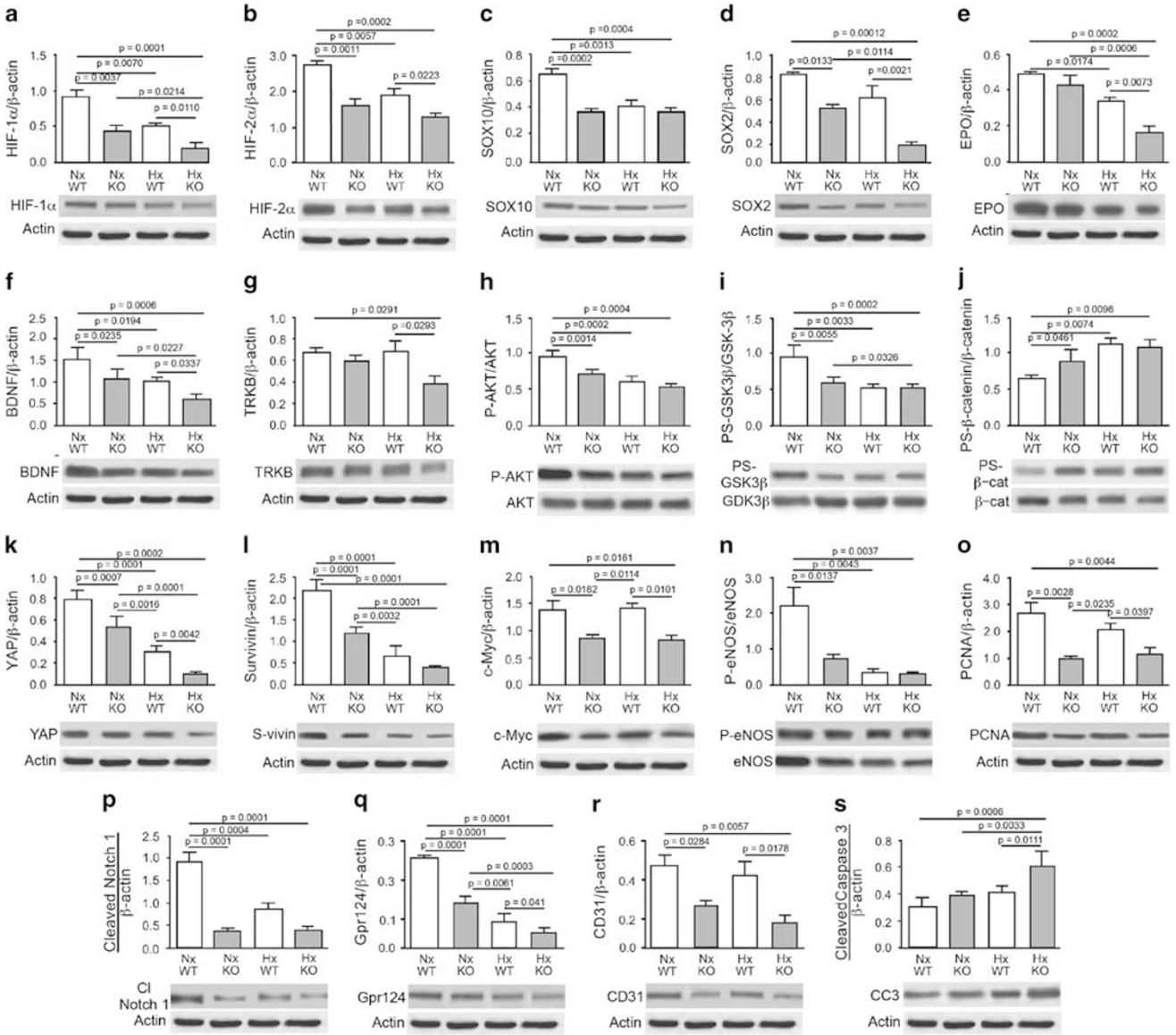

Figure 3 P20 pHIF-1α EC-KO SVZ tissues exhibit decreased expression levels of HIF-1α, HIF-2α, Sox 10, Sox 2, EPO, BDNF, TrkB, phospho (P)-Akt, S_9P-GSK-3β, PS-β-catenin, YAP, Survivin, c-Myc, P-eNOS, PCNA, cleaved Notch 1, Grp124, and CD31 and increases in cleaved caspase-3. Western blot analysis of SVZ tissues derived from normoxic (Nx) and hypoxic (Hx) wild-type (WT) and knockout P20 pups revealed: (**a**) decreased expression of HIF-1α in Hx WT, Nx KO, and Hx KO SVZ (due to the loss of EC HIF-1α in KO pups and the hypoxic insult in Nx pups); (**b**) decreased expression of HIF-2α in Hx WT, Nx KO, and Hx KO SVZ; (**c**) reduced expression of Sox 10 in Hx WT, Nx KO, and Hx KO SVZ; (**d**) reductions in Sox 2 expression in Hx WT and KO SVZ; (**e**) reductions in EPO in HX WT and Hx KO SVZ; (**f**) reductions in BDNF in Nx WT and Nx and Hx KO SVZ; (**g**) reduction of TrkB expression in Hx KO SVZ; (**h**) decreased expression of P-Akt in Hx WT, Nx KO, and Hx KO SVZ; (**i**) decreased expression of S_9P-GSK-3β in Hx WT, Nx KO, and Hx KO SVZ; (**j**) increased expression of PS-β-catenin in Hx WT, Nx KO, and Hx KO SVZ; (**k** and **l**) decreased expressions of YAP and Survivin in Hx WT, Nx KO, and Hx KO SVZ; (**m**) reductions in c-Myc expression in Nx and Hx KO SVZ; (**n**) decreased expression of P-eNOS in Hx WT, Nx KO, and Hx KO SVZ; (**o**) decreased expression of PCNA in Hx WT, Nx KO, and Hx KO SVZ; (**p**) decreased expression of cleaved Notch 1 at P10 in Nx KO, Hx WT, and Hx KO SVZ; (**q** and **r**) decreased Grp124 in Hx WT, Nx KO, and Hx KO SVZ; (**r**) decreased CD31 in Nx KO and Hx KO SVZ; and (**s**) increased expression of cleaved caspase-3 in Hx WT and Hx KO SVZ. Values represent averages of three independent determinations. Horizontal lines denote statistical significance with *P*-values of <0.05. Representative western blots of each of the quantitative western blot analyses are illustrated below each western analysis panel. BDNF, brain-derived neurotrophic factor; EC, endothelial cell; eNOS, endothelial constitutive nitric oxide synthase; EPO, eythropoietin; GSK-3β, glycogen synthase kinase-3β; HIF-1α, hypoxia-inducible factor 1-α, KO, knockout; PCNA, proliferating cell nuclear antigen; SVZ, subventricular zone.

for cleaved caspase-3 expression, confirming the morphological data illustrated in Figures 2h–k. Above the quantitation of the western blot analysis is a representative micrograph of the immunoblot. Figure 2n is comprised of two high-power micrographs of SVZ areas illustrating the decreased cleaved caspase-3 labeling in WT Nx-reared pups compared with the increased labeling in KO pups reared in Nx conditions. Increased cleaved caspase-3 labeling was also noted in WT and KO pups reared in reduced O_2 conditions (not shown).

Immunofluorescence analysis of P10 WT and HIF-1***α*** KO SVZ tissues revealed increased CD31 labeling in WT pups reared in Nx and reduced O_2 conditions, whereas KO pups reared in Nx and reduced O_2 conditions exhibited reduced labeling (Figures 2o–r). Quantitation of CD31-positive SVZ cells reared in these conditions is illustrated in Figure 2s, which shows decreased numbers of CD31-positive cells in KO Nx and reduced O_2 conditions. Interestingly, a modest increase in CD31-positive cells was noted in WT Hx conditions compared with CD31 cell levels in WT Nx conditions. Figure 2t represents the summary of three independent western blot analyses of SVZ tissue lysates, confirming the morphological data illustrated in Figures 2o–r, with the exception of the WT Hx conditions, in which the levels of CD31 were decreased compared with levels observed in WT Nx tissues. This may reflect the contributions of CD31-positive cells in areas adjacent to the SVZ. Above the quantitation of the western blot analysis is a representative micrograph of the immunoblot. Figure 2u is comprised of two high-power micrographs of SVZ areas illustrating the increased Ki67 labeling in WT Nx-reared pups compared with the greatly diminished labeling in KO pups reared in Nx conditions. Increased CD31 labeling was noted in WT pups reared in reduced O_2 conditions, but was relatively diminished in KO pups reared in reduced O_2 conditions (not shown). Supplementary Table 3A is a compilation of the statistical analyses performed on results of the western blots. Supplementary Table 3A is a compilation of the statistical analyses performed on results of the immunofluorescence data and the western blots. Supplementary Table 3B is a summary of the statistical analyses illustrated in Supplementary Table 3A and illustrates the general patterns of gene differences in Nx KO *vs* Hx WT and Nx KO *vs* Hx KO compared with Nx WT *vs* Nx KO, Nx WT *vs* Hx WT, Hx WT *vs* Hx KO, and Hx WT *vs* Hx KO, consistent with differences in the pathways impacted by the various combinations of O_2% and HIF-1***α*** EC KO affecting the cells comprising the SVZ. Similar to our findings in Supplementary Tables 2A and B, when Nx KO, Hx WT, and Hx KO were compared with Nx WT, the KO and Hx samples exhibited decreased expression of genes associated with SVZ cell proliferation. In contrast, Nx KO, HX WT, and Hx KO samples exhibited fewer differences in the decreases (and increase in cleaved caspase-3) in the expression of these genes, consistent with decreased proliferation and increased apoptosis in the SVZ.

HIF-1*α* EC-KO SVZ Tissues Exhibit Decreased Expression Levels of Sox 10, Sox 2, EPO, BDNF, c-Myc, PCNA, P-Akt, Cleaved Notch 1, S_9P-GSK-3*β*, PS-*β*-catenin, P-eNOS, YAP, Survivin, TrkB, Grp124, and CD31 and Increases in Cleaved Caspase-3

Western blot examination of P20 SVZ tissues (comprised of the SVZ immediately lining the lateral ventricles and a small amount of tissue beneath that zone) revealed that endothelial HIF-1*α* deficiency resulted in a significant loss of HIF-1***α*** (Figure 3a) as well as decreased expression levels of HIF-2***α*** (Figure 3b), Sox 10 (Figure 3c), Sox 2 (Figure 3d), EPO (Figure 3e), BDNF (Figure 3f), TRKB in KO Hx tissues (Figure 3g), P-Akt (Figure 3h), S_9P-GSK-3*β* (Figure 3i), increases in PS-*β*-catenin (Figure 3j), decreases in YAP (Figure 3k), Survivin (Figure 3l), c-Myc in KO Nx and KO Hx tissues (Figure 3m), P-eNOS (Figure 3n), PCNA (Figure 3o), cleaved Notch 1 (Figure 3p), Grp124 (Figure 3q), CD31 in KO Nx, and KO Hx tissues (Figure 3r), and increases in cleaved caspase-3 in KO Hx tissues (Figure 3s), consistent with losses of endothelial and neuronal cell densities in the HIF-1***α*** EC-KO mice. Representative western blots used in the quantitation of the proteins listed in this figure are illustrated above the individual panels. Supplementary Table 4A is a compilation of the statistical analyses peformed on results of the western blots.

Supplementary Table 4B is a summary of the statistical analyses illustrated in Supplementary Table 4A and illustrates

Figure 4 SVZ endothelial cells and neural precursors of HIF-1α EC-KO pups exhibit decreased levels of PCNA, Ki67, YAP, and Survivin and increased levels of cleaved caspase-3 (CC3). Immunofluorescence labeling of SVZ tissues of WT and KO P20 pups reared under normoxic (Nx) and hypoxic (Hx) conditions revealed significant differences in PCNA, Ki67, YAP, Survivin, and cleaved caspase-3 expression. WT Nx, WT Hx, KO Nx, and KO Hx P20 SVZ labeled with: (**a**–**d**) CD31 (green fluorescence), PCNA (red fluorescence), and DAPI (blue fluorescence); (**e**–**h**) Nestin (green fluorescence), Ki67 (red fluorescence), and DAPI (blue fluorescence); (**i-l**) CD31 (green fluorescence), YAP (red fluorescence), and DAPI (blue fluorescence); (**m-p**) Nestin (green fluorescence), YAP (red fluorescence), and DAPI (blue fluorescence); (**q-t**) CD31 (green fluorescence), Survivin (red fluorescence), and DAPI (blue fluorescence); (**u-x**) Nestin (green fluorescence), Survivin (red fluorescence), and DAPI (blue fluorescence); (**y-b1**) CD31 (green fluorescence), CC3 (red fluorescence), and DAPI (blue fluorescence); (**c1-f1**) Nestin (green fluorescence), CC3 (red fluorescence), and DAPI (blue fluorescence). Scale bar = 5 μm. BDNF, brain-derived neurotrophic factor; DAPI, 4',6-diamidino-2-phenylindole; EC, endothelial cell; eNOS, endothelial constitutive nitric oxide synthase; EPO, eythropoietin; GSK-3*β*, glycogen synthase kinase-3*β*; HIF-1α, hypoxia-inducible factor 1-α, KO, knockout; PCNA, proliferating cell nuclear antigen; SVZ, subventricular zone; WT, wild type.

general patterns of gene differences in Nx KO *vs* Hx WT and Nx KO *vs* Hx KO compared with Nx WT *vs* Nx KO, Nx WT *vs* Hx WT, Hx WT *vs* Hx KO, and Hx WT *vs* Hx KO, consistent with differences in the pathways impacted by the various combinations of O_2% and HIF-1***α*** EC KO affecting the cells comprising the SVZ. Similar to our findings in

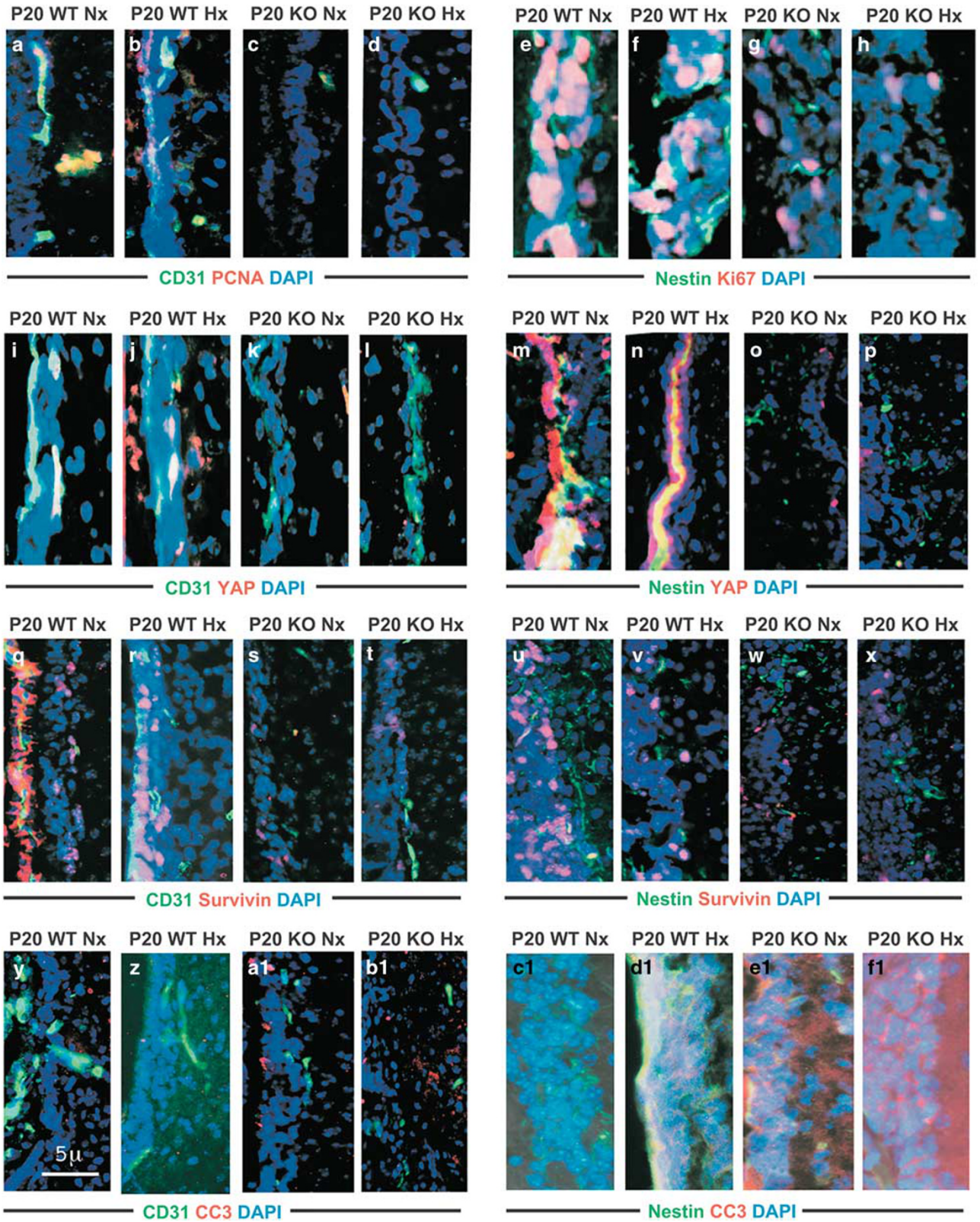

Supplementary Tables 2A, B and 3A,B, when Nx KO, Hx WT, and Hx KO were compared with Nx WT, the KO and Hx samples exhibited decreased expression of genes associated with SVZ cell proliferation and increases in cleaved caspase-3 consistent with apoptosis. In contrast, Nx KO, Hx WT, and Hx KO samples exhibited fewer differences in the decreases (and increase in cleaved caspase-3) in expression of these genes, consistent with decreased proliferation and increased apoptosis in the SVZ.

SVZ of HIF-1α EC-KO Pups Exhibit Decreased Levels of PCNA, Ki67, YAP, and Survivin and Increased Levels of Cleaved Caspase-3

Immunofluorescence analysis of SVZ harvested from P20 WT and HIF-1α EC-KO pups reared under Nx and Hx (reduced O_2 (10%)) conditions revealed similar changes in the expression levels of PCNA in CD31-positive ECs and Ki67 in Nestin-positive neural cells. Specifically, ECs in the SVZ harvested from WT pups reared under Nx and Hx conditions exhibited occasional PCNA labeling (magenta and white labeling due to colocalization with DAPI and ECs) (Figures 4a and b), whereas the SVZ harvested from KO pups reared under Nx and Hx conditions exhibited essentially non-detectable PCNA labeling, and a relative paucity of CD31-positive cells (Figures 4c and d). Similarly, Nestin-positive cells in the SVZ harvested from WT pups reared under Nx and Hx conditions exhibited robust Ki67 labeling, colocalizing with Nestin (Figures 4e and f), whereas the SVZ harvested from KO pups reared under Nx and Hx conditions exhibited only occasional Ki67 labeling (Figures 4g and h).

YAP labeling in both CD31- and Nestin-positive SVZ cells essentially mirrored what was observed in the PCNA and Ki67 labeling. Namely, ECs in the SVZ harvested from WT pups reared under Nx and Hx conditions exhibited occasional YAP labeling (Figures 4i and j), whereas the SVZ harvested from KO pups reared under Nx and Hx conditions exhibited essentially non-detectable YAP labeling (Figures 4k and l). Similarly, Nestin-positive cells in the SVZ harvested from WT pups reared under Nx and Hx conditions exhibited robust YAP labeling (Figures 4m and n), whereas the SVZ harvested from KO pups reared under Nx and Hx conditions exhibited essentially non-detectable YAP labeling (Figures 4o and p).

Survivin labeling in both CD31- and Nestin-positive SVZ cells also mirrored what was observed in the PCNA and Ki67 and YAP labeling. CD31-positive ECs in the SVZ harvested from WT pups reared under Nx conditions exhibited robust Survivin labeling (Figures 4q and r), whereas cells from KO pups reared under Hx conditions exhibited rare Survivin- and CD31-positive cells (Figures 4s and t). Nestin-positive cells from the SVZ harvested from KO pups reared under Nx conditions exhibited occasional Survivin positivity, whereas only rare Nestin- and Survivin-positive cells were observed in the SVZ of KO pups reared under Hx conditions (Figures 4u and x).

Cleaved caspase-3 labeling in CD31-positive SVZ cells harvested from WT pups and reared under Nx and Hx conditions exhibited essentially no detectable labeling (Figures 4y and z). In contrast, cleaved caspase-3 labeling in CD31-positive SVZ cells harvested from KO pups and reared under Nx and Hx conditions exhibited occasional labeling (Figures 4A1 and B1). While Nestin-positive cells from the SVZ harvested from WT pups reared under Nx conditions exhibited no detectable cleaved caspase-3 positivity (Figure 4 C1), cleaved caspase-3 labeling was observed in the SVZ of Hx-reared WT pups (Figure 4D1). KO pup Nx- and Hx-reared SVZ exhibited modest labeling (Figures 4E1 and F1).

In general, our immunofluorescence data confirms our western blotting data, illustrating that the SVZ decreased PCNA and Ki67 expression in the endothelial and neuronal compartments in KO samples, respectively. Similarly, YAP and Survivin expression were also decreased in the endothelial and neuronal compartments in KO samples. Last, increased cleaved caspase-3 expression was noted in both the endothelial and neuronal compartments of SVZ tissues in KO samples.

HIF-1α EC-KO Hippocampal Dentate Gyrus Tissues Exhibit the Absence of Vascular HIF-1α Expression and Decreased Ki67 Expression Compared with WT-Derived Hippocampal Tissues

Immunofluorescence examination of the dentate gyrus of P20 WT and KO pups reared under Nx and Hx conditions revealed an absence of vascular HIF-1α expression in the KO Nx and Hx tissues (Figures 5a–d and Figures 5c and d), compared with the robust vascular pattern staining in Nx WT tissue (Figure 5a, green fluorescence). HIF-1α expression in Hx WT tissue was present, but diminished compared with the Nx WT expression (compare Figures 5a and b). DCX staining marks the granular layer (Figures 5a–d, red fluorescence). Proliferation in the dentate gyrus at P20 was assessed using Ki67 labeling (red fluorescence) and DAPI staining to demarcate granular cell nuclei (blue fluorescence). GFAP-expressing cells were noted by green fluorescence. Markedly decreased proliferation was noted in the granular layer in Hx WT tissue (Figure 5f) compared with that noted in Nx WT tissues (Figure 5e). In contrast, no detectable Ki67 labeling was noted in Nx KO and Hx KO (Figures 5g and h). These differences were confirmed by quantitation of the areas (in pixels) of Ki67-positive cells assessed at P10 (micrographs not shown) (Figure 5i) and P20 (Figure 5j).

The analysis of the dentate gyrus, the other known neurogenic zone of the brain, allowed for confirmation of our findings in the SVZ.

Behavioral Studies of HIF-1α EC-KO Pups

When open field activities were assessed at P20 comparing KO and WT pups with males and females grouped together, no statistically significant differences in total distance, distance/move, mean velocity, rest time, margin distance, margin time, center distance, and center time were observed

(data not shown). However, when male and female pups were examined separately and compared, several statistically significant differences were noted (Figures 6a–h). Specifically, HIF-1α EC-KO male pups reared under Nx conditions exhibited increased center time (Figure 6a), center distance (Figure 6b) and decreased margin distance (Figure 6c) and

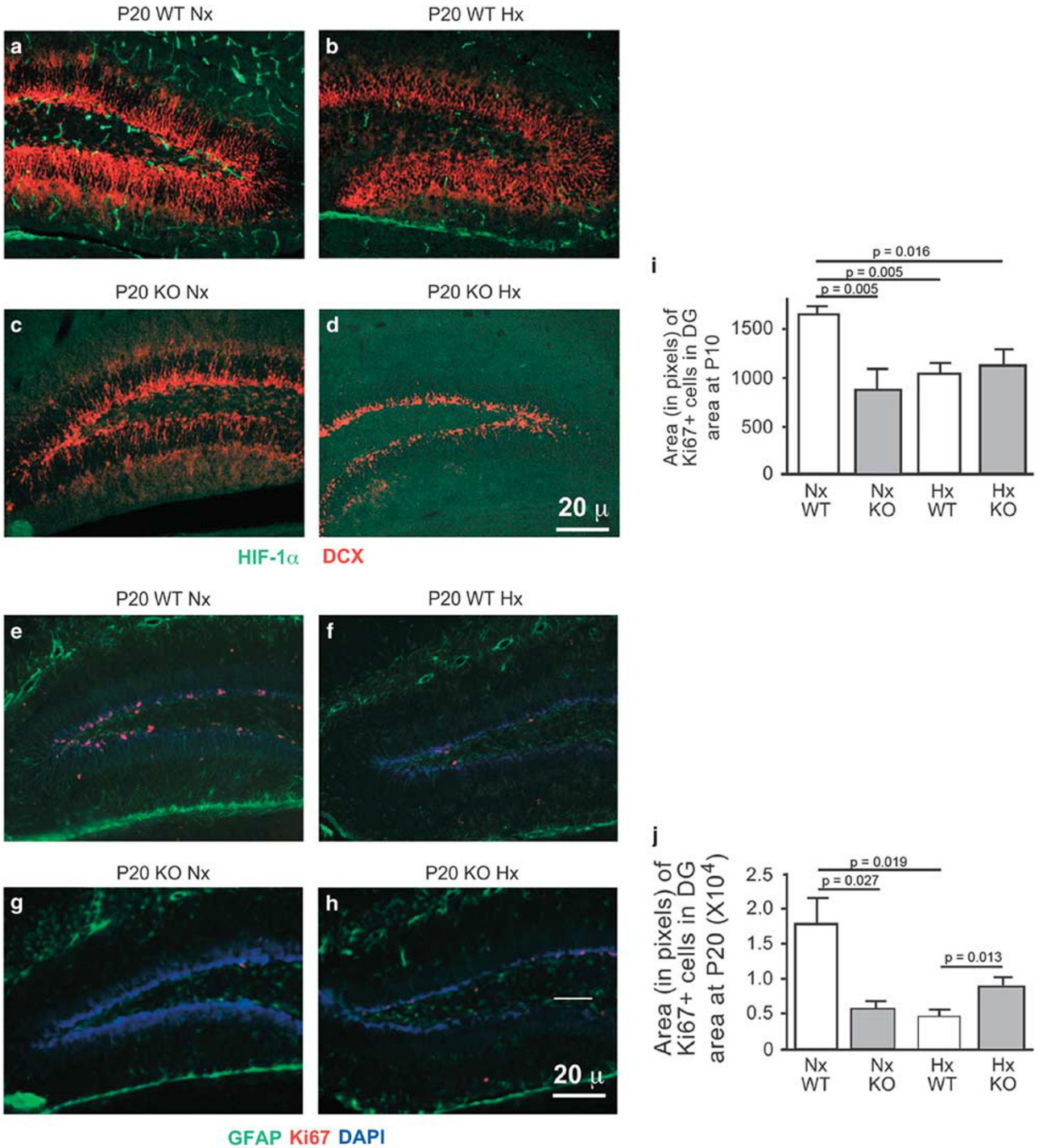

Figure 5 HIF-1α EC-KO dentate gyrus tissues exhibit absence of vascular HIF-1α expression and decreased Ki67 expression compared with WT-derived hippocampal tissues. Immunofluorescence labeling of hippocampal tissues of WT and KO P20 pups reared under normoxic (Nx) and hypoxic (Hx) conditions revealed an absence of vascular HIF-1α expression in KO tissues and significant reduction in Ki67 expression in the granular layer of the dentate gyrus (DG). (**a**) WT Nx, (**b**) WT Hx, (**c**) KO Nx, and (**d**) KO Hx. HIF-1α = green fluorescence; doublecortin (DCX) = red fluorescence. (**e**) WT Nx; (**f**) WT Hx, (**g**) KO E Nx, and (**h**) KO Hx. GFAP = green fluorescence; Ki67 = red fluorescence; DAPI = blue fluorescence. (**i** and **j**) Quantitation of the areas (in pixels) of Ki67-positive cells assessed at P10 (**i**) and P20 (**j**). Horizontal lines denote statistical significance with *P*-values of <0.05, $n=3$. DAPI, 4',6-diamidino-2-phenylindole; GFAP, glial fibrillary acidic protein; HIF-1α, hypoxia-inducible factor 1-α, KO, knockout; SVZ, subventricular zone; WT, wild type.

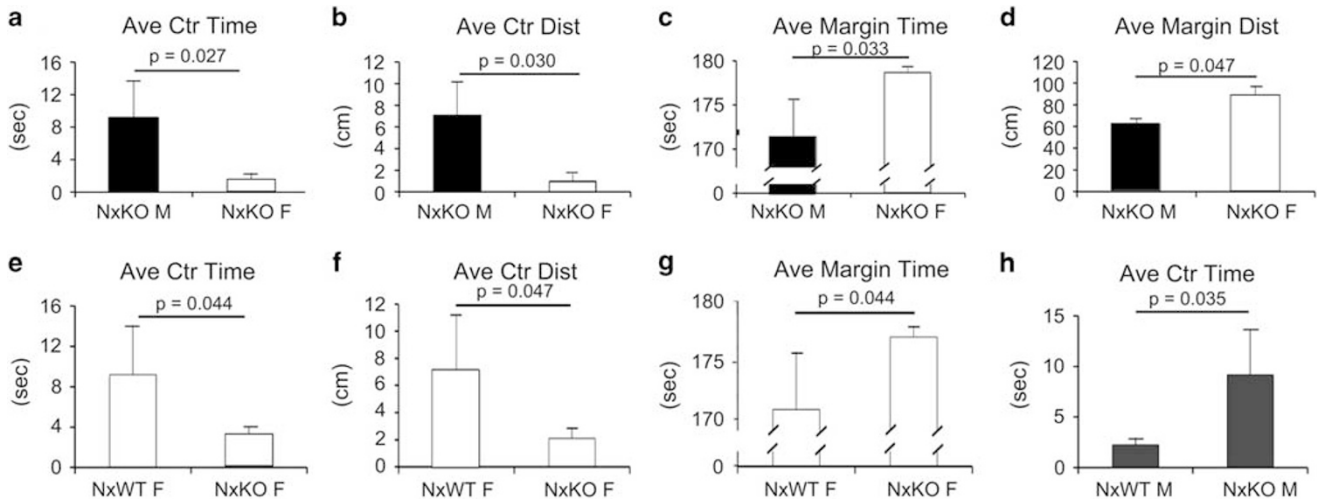

Figure 6 Behavior studies performed at P20 (open field activity test) reveal statistically significant differences in wild-type (WT) and knockout (KO) mice in a gender-specific manner. Thirty-seven male and female P20 pups (20 HIF-1α EC-KO and 17 WT C57BL/6 littermate pups, comprised of 18 normoxic (Nx)-reared and 19 hypoxic (Hx)-reared pups totaling 17 males—8 Nx and 9 Hx males (black boxes) and 20 females—10 Hx and 10 Nx females (white boxes) were evaluated for spontaneous open field behavior (**a**–**d**). (**a**) Average center (Ave Ctr) times, (**b**) average center distances (Ave Ctr Dist), (**c**) average (Ave) margin times, and (**d**) average margin distances of Nx KO males (Nx KO M) and Nx KO females (Nx KO F) illustrating the decreased center times and distances of the KO female pups (**a** and **b**) and the reciprocal increased margin times and margin distances of the females (**c** and **d**) compared with males. (**e**–**h**) (**e**) Average center times, (**f**) average center distances, and (**g**) average margin times of Nx WT females (Nx WT F) and Nx KO females (Nx KO F) illustrating the decreased center times and distances of the KO female pups (**e** and **f**) and the reciprocal increased margin times and distances of the KO females (**g**) compared with WT females. (**h**) Average center time of Nx WT males (Nx WT M) and Nx KO males (Nx KO M) illustrating the decreased center times of the KO males, which are in contrast to the Nx WT and KO females (**e**). Each group was comprised of at least three and no more than 10 pups. Horizontal lines denote statistical significance with *P*-values of <0.05.

margin time (Figure 6d), compared with their KO female littermates.

When WT and HIF-1α EC-KO female pups were compared under Nx conditions, WT female pups exhibited increased average center times (Figure 6e) and average center distances (Figure 6f) and decreased average margin times (Figure 6g), compared with HIF-1α KO female pups. In contrast, when WT and HIF-1α EC-KO male pups were compared under Nx conditions, WT male pups exhibited decreased average center times compared with male HIF-1α KO pups (Figure 6h). Additionally, a comparison of the average center times of Nx WT females and males also revealed differences, with the Nx WT females having 9.2 ± 4.9 s of center time, whereas the Nx WT males exhibited 1.6 ± 0.6 s of center time with a $P = 0.038$.

These studies illustrate the gender-specific effects of the presence and absence of EC HIF-1α on specific behaviors in C57BL/6 mice.

DISCUSSION

EC—neural precursor interactions in the neurogenic zones of the brain (the SVZ and the hippocampus)—have been a topic of interest for several years, being investigated in a wide range of species using a plethora of techniques.[11,14,31–35] For the past several years, we have been investigating selected aspects of endothelial–neuronal precursor interactions using both *in vitro* and *in vivo* murine models. In a series of *in vitro* studies, we demonstrated that NPC establish intimate contacts with EC and elicit robust vascular tube formation and maintenance mediated by induction of vascular VEGF and BDNF by NPC NO. In turn, the VEGF and BDNF activate EC and NPC VEGFR2 and TrkB. The NPC respond to VEGF and BDNF with increased proliferation and activation of eNOS and generation of NO consistent with an inducible feedback signaling loop between the EC and NPC.[11,16,17] Later studies expanded our appreciation of the growth factors and signaling pathways involved in modulating the behaviors of these neurogenic zones.[2,3,10,12,17,24] Selected transcription factors (HIF-1α), enzymes that regulate HIF-1α activity (PHD2), and additional growth factors including SDF-1 and its receptor CXCR4 were shown to be involved as well as components of the PI3K pathway including Akt, mTOR, p-p70, p-Elf4E, and p-4E-BP1.[2,3] Further investigations confirmed a role of GSK-3β as an important signaling node in the modulation of the EC and NPC comprising the neurovascular niche.[12] In recent studies, we have discovered that a Sox family member, Sox 10, has an important role in the development, maintenance, and responsiveness of the SVZ, regulating a number of genes that in turn are involved in NPC biology.[10,24] Sox 10 was found to be upstream of HIF-1α and several growth factors and proteins were known to be involved in endothelial and neural cell behaviors. Our *in vitro* data correlated well with our *in vivo* studies in which the biochemical data was in good agreement with our tissue

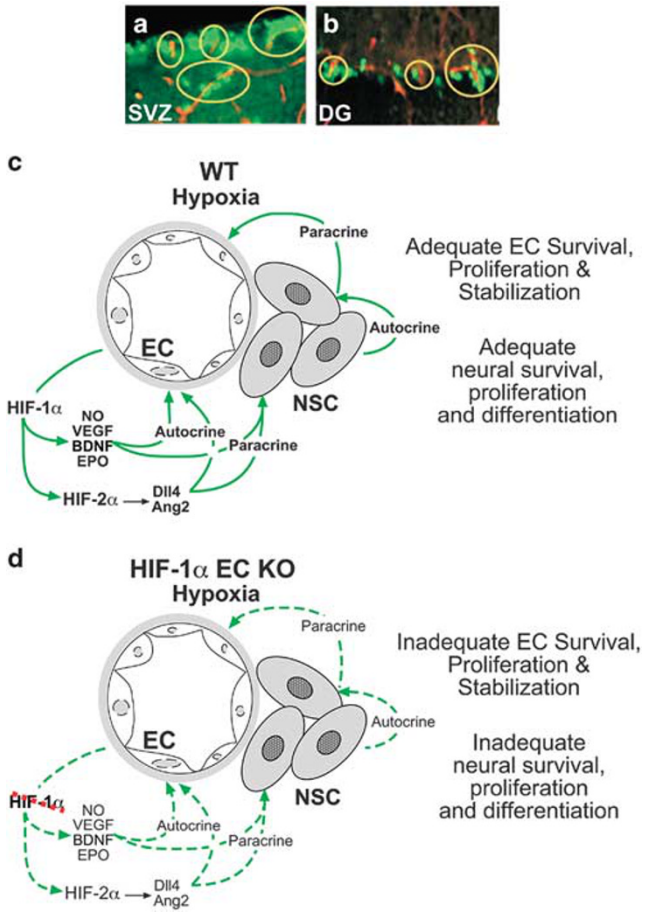

Figure 7 Schematic representation of our proposed model of dynamic signaling between the microvasculature and neuronal precursors resident in the subventricular zone (SVZ) and dentate gyrus (DG). (**a** and **b**) Representative high-power immunofluorescence micrographs illustrating the intimate relationships between the microvasculature (EC) and neuronal precursors (NPC) in the subventricular zone (SVZ) (**a**) and the dentate gyrus (DG) (**b**). Endothelial cells = CD31-positive Red fluorescence; neuronal precursors = Nestin-positive—green fluorescence. (**c**) Schematic depicting hypoxia-driven hypoxia-inducible factor 1-α (HIF-1α)-mediated signaling in the SVZ and DG niches involving induction of HIF-1α, HIF-2α, and downstream factors and their pathway components (listed in Figure 4), affecting both neural stem cells (NSCs) and ECs (denoted by solid green arrows and bold type) in autocrine and paracrine receptor-mediated pathways. (**d**) Schematic depicting hypoxia-driven HIF-1α-mediated signaling in the SVZ and DG niches in the absence of HIF-1α illustrating the effects of the absence of EC HIF-1α on downstream factors and their pathway components (listed in Figure 4), affecting both NSCs and ECs (denoted by dashed green arrows and plain type) in autocrine and paracrine receptor-mediated pathways. The schemes represented in panels (**c** and **d**) were generated from data presented in this study and previous studies.[2,3,10–12,24] BDNF, brain-derived neurotrophic factor; DG, dentate gyrus; EC, endothelial cell; EPO, eythropoietin; HIF-1α, hypoxia-inducible factor 1-α; KO, knockout; NO, nitric oxide; SVZ, subventricular zone; VEGF, vascular endothelial growth factor; WT, wild type.

culture data and both were consistent with our behavioral data.[2,3,10,15,18,24] Interestingly, we noted significant strain differences in our comparisons of C57BL/6 and CD1 mice mimicking the range of responsiveness and recovery from Hx insult in the very premature.[2,3] To further study the importance of endothelial HIF-1***α*** in the poor responding premature newborn, we elected to study its role in the recovery process in C57BL/6 pups, being a strain that exhibits a poor Sox 10/HIF-1***α*** response to Hx insult compared with the CD1's robust response.[2,3,10,12,24] Our current data illustrates that conditions which result in either decrease (Hx insult) and/or loss (HIF-1***α*** EC KO) of HIF-1***α*** in C57BL/6 pups elicit similar responses in proliferation (decrease) and apoptosis (increase) of endothelial and neuronal cell populations in the SVZ.

C57BL/6 HIF-1*α* EC-KO mice have been previously used to investigate the roles of EC HIF-1***α*** in the responsiveness of a variety of organs and tissues to the Hx environment.[26,36–40] The C57BL/6 HIF-1***α*** EC-KO mice that were generated were devoid of endothelial HIF-1***α*** expression and the KO EC exhibited decreased expression of BDNF, eNOS, p-Akt, inactive GSK-3*β* and increased serine phosphorylated *β*-catenin, consistent with the decreased proliferation rate and increased apoptosis observed in the SVZ and DG of KO animals.

Western blot analysis of ECs derived from HIF-1*α* EC-KO mice revealed decreased HIF-2***α*** expression in both Nx and reduced O_2 conditions. Studies have demonstrated that in ECs tested, HIF-1***α*** and HIF-2***α*** have complex, complementary, non-overlapping functions in angiogenesis.[41–45] In recent studies, investigators have documented differential regulation of HIF-***α*** subunits in macrophages and PC12 cells driven by hypoxia and redox balance.[46–49] Our finding of decreased HIF-2***α*** expression in HIF-1***α*** KO EC suggests that there may be a regulation of HIF-***α*** isoforms, possibly mediated via modulation of HIF-*α* subunit specificities of prolyl hydroxylases.[50]

Further, western blotting data of lysates of SVZ tissues of KO animals exhibited decreased Sox 10 and 2, EPO, and BDNF, consistent with decreased p-Akt, inactive GSK-3*β*, and increased SP-*β*-catenin. These changes denote reductions in signaling pathways, resulting in decreased proliferation and increased apoptosis as evidenced by decreased TrkB, cleaved Notch 1, phospho-eNOS, PCNA, and Survivin, YAP, Grp124, and CD31 and increased cleaved caspase-3. These biochemical changes were confirmed by immunofluorescence microscopy data illustrating SVZ tissue expression of PCNA, Ki67, YAP Survivin, and cleaved caspase-3 in EC and NPC. Last, the absence of EC HIF-1***α*** in the DG was confirmed by immunofluorescence as was its correlation with a loss of granular cell proliferation in the granular zone of the DG.

These findings illustrate the importance of EC HIF-1***α*** in the response to and recovery from sublethal chronic hypoxia and the roles the SVZ and DG ECs have in not only EC responses but also in the responses of SVZ and DG neuronal precursor cells to Hx insults. Thus, we postulate that SVZ and DG endothelial responsiveness to Hx insult not only affects the resident microvasculature but also has significant effects on resident neuronal precursors, which in turn may have

profound effects on cognitive and motor function. Specifically, as illustrated in Figure 7, in WT Hx conditions hypoxia-driven HIF-1α mediates signaling in the SVZ and DG niches involving induction of Sox 10, HIF-1α, HIF-2α, and downstream factors and their pathway components, affecting both NSCs and ECs (denoted by solid green arrows and bold type) in autocrine and paracrine receptor-mediated pathways. In contrast, in HIF-1α EC-KO mice, hypoxia-driven HIF-1α-mediated signaling in the SVZ and DG niches is absent, affecting the induction of downstream factors and their pathway components, which in turn affect both NSCs and ECs (denoted by dashed green arrows and plain type) autocrine and paracrine receptor-mediated pathways.

Consistent with our biochemical and immunofluorescence data and analyses, the results of the open field activity tests illustrate that there are gender differences in the response to Hx insult with the loss of EC HIF-1α compared with WT littermate pups. In previous studies, we had restricted our behavioral studies to males. However, in light of recent studies documenting sex differences in the response to treatments in premature newborns in which investigators documented an increased incidence, injury, and death in premature males compared with premature females of the same gestational age, as well as differences in the prevalence of cognitive, neurologic, and behavioral deficits in boys and girls born extremely premature when examined at 10 years of age (with boys having higher prevalences of these deficits),[51–56] and mixed results in Fragile X studies,[57,58] we decided to assess the responses of both males and females. Our data are consistent with the concept that males and females exhibit different behaviors, with Nx KO males exhibiting increased center time and center distance compared with female littermates, suggesting differences in anxiety levels. Interestingly, comparing Nx WT females with males, we noted increased center time in Nx WT females, whereas Nx WT males exhibited decreased center time. These data suggest that while Nx WT females are less anxious than their Nx WT male littermates, under HIF-1α EC-KO conditions, males appear less anxious than their littermate females, suggesting the possibility of differential signaling pathway(s) component expression levels and engagement(s) in males and females, resulting in differential behavioral outcomes.

These studies demonstrate the important effect of EC HIF-1α modulating the proliferative and apoptotic behaviors of EC and NPC in the neurogenic regions of the brain and the sex-specific behavioral responses of these mice in Nx and Hx settings. Further, these studies underscore the importance of taking into account sex-specific responses in the design, treatment and evaluation of animal models and patients following injury, during treatment, and in assessing outcomes.

Supplementary Information accompanies the paper on the Laboratory Investigation website (http://www.laboratoryinvestigation.org)

ACKNOWLEDGMENTS

We express our thanks to Dr Laura R Ment for her thoughtful comments. This work was supported, in part, by USPHS Grant, PO1-NS00344738, a Reed Foundation Fellowship and a generous gift from Joseph and Lucille Madri (to JAM); USPHS Grant RO1-HL075616 (to FG); and USPHS Grant PO1-NS00344738 (to MS).

DISCLOSURE/CONFLICT OF INTEREST

The authors declare no conflict of interest.

1. Ment LR, Vohr B, Allan W, *et al.* Change in cognitive function over time in very low-birth-weight infants. JAMA 2003;289:705–711.
2. Li Q, Michaud M, Stewart W, *et al.* Modeling the neurovascular niche: murine strain differences mimic the range of responses to chronic hypoxia in the premature newborn. J Neurosci Res 2008;86:1227–1242.
3. Li Q, Liu J, Michaud M. *et al.* Strain differences in behavioral and cellular responses to perinatal hypoxia and relationships to neural stem cell survival and self-renewal: modeling the neurovascular niche. Am J Pathol 2009;175:2133–2146.
4. Wilson-Costello D, Friedman H, Minich N, *et al.* Improved survival rates with increased neurodevelopmental disability for extremely low birth weight infants in the 1990s. Pediatrics 2005;115:997–1003.
5. Tyson JE, Saigal S. Outcomes for extremely low-birth-weight infants: disappointing news. JAMA 2005;294:371–373.
6. Saigal S, Doyle LW. An overview of mortality and sequelae of preterm birth from infancy to adulthood. Lancet 2008;371:261–269.
7. Saigal S, Stoskopf B, Streiner D, *et al.* Transition of extremely low-birth-weight infants from adolescence to young adulthood: comparison with normal birth-weight controls. JAMA 2006;295:667–675.
8. Hack M, Flannery DJ, Schluchter M, *et al.* Outcomes in young adulthood for very-low-birth-weight infants. N Engl J Med 2002; 346:149–157.
9. Curristin SM, Cao A, Stewart WB, *et al.* Disrupted synaptic development in the hypoxic newborn brain. Proc Natl Acad Sci USA 2002;99: 15729–15734.
10. Li Q, Canosa S, Flynn K, *et al.* Modeling the neurovascular niche: unbiased transcriptome analysis of the murine subventricular zone in response to hypoxic insult. PLoS One 2013;876265.
11. Li Q, Ford MC, Lavik EB, *et al.* Modeling the neurovascular niche: VEGF- and BDNF-mediated cross-talk between neural stem cells and endothelial cells: an *in vitro* study. J Neurosci Res 2006;84:1656–1668.
12. Li Q, Michaud M, Canosa S, *et al.* GSK-3β: a signaling pathway node modulating neural stem cell and endothelial cell interactions. Angiogenesis 2011;14:173–185.
13. Madri JA. Modeling the neurovascular niche: implications for recovery from CNS injury. J Physiol Pharmacol 2009;60(Suppl 4):95–104.
14. Lavik E, Madri JA. Angiogenesis, The Neurovascular Niche and Neuronal Reintegration After Injury. Springer: The Netherlands, 2011.
15. Ford MC, Bertram JP, Hynes SR, *et al.* A macroporous hydrogel for the coculture of neural progenitor and endothelial cells to form functional vascular networks *in vivo*. Proc Natl Acad Sci USA 2006;103:2512–2517.
16. Rauch MF, Michaud M, Xu H, *et al.* Primary neural progenitor and endothelial cells in a macroporous gel promote stable vascular networks *in vivo*. J Biomater Sci Polym Ed 2008;19:1469–1485.
17. Williams C, Rauch MF, Michaud M, *et al.* Short term interactions with long term consequences: modulation of chimeric vessels by neural progenitors. PLoS One 2012;7:e53208.
18. Rauch MF, Hynes SR, Bertram J, *et al.* Engineering angiogenesis following spinal cord injury: a coculture of neural progenitor and endothelial cells in a degradable polymer implant leads to an increase in vessel density and formation of the blood-spinal cord barrier. Eur J Neurosci 2009;29:132–145.
19. Chow J, Ogunshola O, Fan SY, *et al.* Astrocyte-derived VEGF mediates survival and tube stabilization of hypoxic brain microvascular endothelial cells *in vitro*. Brain Res Dev Brain Res 2001;130:123–132.
20. Ment LR, Stewart WB, Fronc R, *et al.* Vascular endothelial growth factor mediates reactive angiogenesis in the postnatal developing brain. Dev Brain Res 1997;100:52–61.
21. Ment LR, Stewart WB, Scaramuzzino D, *et al.* An *in vitro* three-dimensional coculture model of cerebral microvascular angiogenesis and differentiation. In Vitro Cell Dev Biol Anim 1997;33:684–691.

22. Ogunshola OO, Antic A, Donoghue MJ, *et al.* Paracrine and autocrine functions of neuronal vascular endothelial growth factor (VEGF) in the central nervous system. J Biol Chem 2002;277:11410–11415.
23. Ogunshola OO, Stewart WB, Mihalcik V, *et al.* Neuronal VEGF expression correlates with angiogenesis in postnatal developing rat brain. Brain Res Dev Brain Res 2000;119:139–153.
24. Li Q, Tsuneki M, Krauthammer M, *et al.* Modulation of Sox10, HIF-1*α*, Survivin and YAP by minocycline in the treatment of neurodevelopmental handicaps following hypoxic insult. Am J Pathol 2015;185: 2364–2378.
25. Kisanuki YY, Hammer RE, Miyazaki J, *et al.* Tie2-Cre transgenic mice: a new model for endothelial cell-lineage analysis *in vivo*. Dev Biol 2001;230:230–242.
26. Ryan HE, Lo J, Johnson RS. HIF-1 alpha is required for solid tumor formation and embryonic vascularization. EMBO J 1998;17:3005–3015.
27. Fagel DM, Ganat Y, Silbereis J, *et al.* Cortical neurogenesis enhanced by chronic perinatal hypoxia. Exp Neurol 2005;199:77–91.
28. Graesser D, Solowiej A, Bruckner M, *et al.* Altered vascular permeability and early onset of experimental autoimmune encephalomyelitis in PECAM-1-deficient mice. J Clin Invest 2002;109:383–392.
29. Flynn KM, Michaud M, Madri JA. CD44 deficiency contributes to enhanced experimental autoimmune encephalomyelitis: a role in immune cells and vascular cells of the blood–brain barrier. Am J Pathol 2013;182:1322–1336.
30. Flynn KM, Michaud M, Canosa S, *et al.* CD44 regulates vascular endothelial barrier integrity via a PECAM-1 dependent mechanism. Angiogenesis 2013;16:89–705.
31. Louissaint A, Rao S, Leventhal C, *et al.* Coordinated interaction of neurogenesis and angiogenesis in the adult songbird brain. Neuron 2002;34:945–960.
32. Palmer TD, Willhoite AR, Gage FH. Vascular niche for adult hippocampal neurogenesis. J Comp Neurol 2000;425:479–494.
33. Pereira AC, Huddleston DE, Brickman AM, *et al.* An in vivo correlate of exercise-induced neurogenesis in the adult dentate gyrus. Proc Natl Acad Sci USA 2007;104:5638–5644.
34. Tavazoie M, Van der Veken L, Silva-Vargas V, *et al.* A specialized vascular niche for adult neural stem cells. Cell Stem Cell 2008;3:279–288.
35. Shen Q, Goderie SK, Jin L, *et al.* Endothelial cells stimulate self-renewal and expand neurogenesis of neural stem cells. Science 2004;304: 1338–1340.
36. Ueno M, Tomita S, Nakagawa T, *et al.* Effects of aging and HIF-1alpha deficiency on permeability of hippocampal vessels. Microsc Res Technol 2006;69:29–35.
37. Branco-Price C, Zhang N, Schnelle M, *et al.* Endothelial cell HIF-1*α* and HIF-2*α* differentially regulate metastatic success. Cancer Cell 2012;21:52–65.
38. Huang Y, Lei L, Liu D, *et al.* Normal glucose uptake in the brain and heart requires an endothelial cell-specific HIF-1*α*-dependent function. Proc Natl Acad Sci USA 2012;109:17478–17483.
39. Sim J, Johnson RS. A whiter shade of gray: HIF and coordination of angiogenesis with postnatal myelination. Dev Cell 2014;30:116–117.
40. Kalucka J, Schley G, Georgescu A, *et al.* Kidney injury is independent of endothelial HIF-1*α*. J Mol Med (Berl) 2015;93:891–904.
41. Ohneda O, Nagano M, Fujii-Kuriyama Y. Role of hypoxia-inducible factor-2alpha in endothelial development and hematopoiesis. Methods Enzymol 2007;435:199–218.
42. Sowter HM, Raval RR, Moore JW *et al.* Predominant role of hypoxia-inducible transcription factor (Hif)-1alpha versus Hif-2alpha in regulation of the transcriptional response to hypoxia. Cancer Res 2003;63: 130–6134.
43. Skuli N, Simon MC. HIF-1alpha versus HIF-2alpha in endothelial cells and vascular functions: is there a master in angiogenesis regulation? Cell Cycle 2009;8:3252–3253.
44. Skuli N, Liu L, Runge A, *et al.* Endothelial deletion of hypoxia-inducible factor-2alpha (HIF-2alpha) alters vascular function and tumor angiogenesis. Blood 2009;114:469–477.
45. Skuli N, Majmundar AJ, Krock BL, *et al.* Endothelial HIF-2*α* regulates murine pathological angiogenesis and revascularization processes. J Clin Invest 2012;122:427–1443.
46. Yuan G, Peng YJ, Reddy VD, *et al.* Mutual antagonism between hypoxia-inducible factors 1*α* and 2*α* regulates oxygen sensing and cardio-respiratory homeostasis. Proc Natl Acad Sci USA 2013;110: 1788–E1796.
47. Poitz DM, Augstein A, Hesse K, *et al.* Regulation of the HIF-system in human macrophages—differential regulation of HIF-*α* subunits under sustained hypoxia. Mol Immunol 2014;57:226–235.
48. Weidemann A, Johnson RR. Biology of HIF-1alpha. Cell Death Differ 2008;15:621–627.
49. Tormos KV, Chandel NS. Inter-connection between mitochondria and HIFs. J Cell Mol Med 2010;14:795–804.
50. Appelhoff RJ, Tian YM, Raval RR *et al.* Differential function of the prolyl hydroxylases PHD1, PHD2, and PHD3 in the regulation of hypoxia-inducible factor. J Biol Chem 2004;279:38458–38465.
51. Skiöld B, Alexandrou G, Padilla N *et al.* Sex differences in outcome and associations with neonatal brain morphology in extremely preterm children. J Pediatr 2014;164:1012–1018.
52. Cohen. SS, Stonestreet BS. Sex differences in behavioral outcome following neonatal hypoxia ischemia: Insights from a clinical meta-analysis and a rodent model of induced hypoxic ischemic injury. Exp Neurol 2014;256:70–73.
53. Månsson J, Fellman V, Stjernqvist K, *et al.* Extremely preterm birth affects boys more and socio-economic and neonatal variables pose sex-specific risks. Acta Paediatr 2015;104:514–521.
54. Smith AL, Alexander M, Rosenkrantz TS, *et al*. Sex differences in behavioral outcome following neonatal hypoxia ischemia: insights from a clinical meta-analysis and a rodent model of induced hypoxic ischemic brain injury. Exp Neurol 2014;254:54–67.
55. Peacock JL, Marston L, Marlow N, *et al.* Neonatal and infant outcome in boys and girls born very prematurely. Pediatr Res 2012;71: 305–310.
56. Kuban KC, Joseph RM, O'Shea TM, *et al*. Extremely Low Gestational Age Newborn (ELGAN) Study Investigators Girls and boys born before 28 weeks gestation: risks of cognitive, behavioral, and neurologic outcomes at age 10 years. J Pediatr 2016;173:69–75.
57. Bilousova TV, Dansie L, Ngo M, *et al.* Minocycline promotes dendritic spine maturation and improves behavioural performance in the fragile X mouse model. J Med Genet 2013;46:94–102.
58. Papapetropoulos A, Desai KM, Rudic RD, *et al.* Nitric oxide synthase inhibitors attenuate transforming-growth-factor-beta 1-stimulated capillary organization *in vitro*. Am J Pathol 1997;150: 1835–1844.